Journal of Catalysis 284 (2011) 68–76

Contents lists available at SciVerse ScienceDirect

Journal of Catalysis

journal homepage: www.elsevier.com/locate/jcat

Biomimetic catalysis at silicon centre using molecularly imprinted polymers

Vincenzo Abbate [a,*], Alan R. Bassindale [a], Kurt F. Brandstadt [b], Peter G. Taylor [a,*]

[a] Department of Chemistry and Analytical Sciences, The Open University, Walton Hall, Milton Keynes MK7 6AA, UK
[b] Dow Corning Corporation, 2200 W Salzburg Rd., Midland, MI 48686, USA

ARTICLE INFO

Article history:
Received 12 April 2011
Revised 29 August 2011
Accepted 31 August 2011
Available online 6 October 2011

Keywords:
Biomimetic catalyst
Molecularly imprinted polymers
Transition state
Siloxane bond
Silica precipitation

ABSTRACT

The first example of biomimetic siloxane bond formation catalyzed by molecularly imprinted polymers (MIPs) is reported. MIPs were prepared by free-radical polymerization and characterized via a combination of solid-state NMR, infrared spectroscopy, and electron microscopy studies. Methacrylic acid–based polymers with high functional monomer content were observed to catalyze the hydrolysis and condensation of a model monoalkoxysilane to a greater extent when compared with the corresponding blank (non-imprinted) materials and buffer control solutions, as judged by quantitative gas chromatography investigations. Moreover, the polymers were used as biomimetic catalysts to synthesize silica-MIP hybrids with a certain degree of control of the microstructure of the resulting composites.

1. Introduction

Molecular imprinting is perhaps the most recent example of biomimetic chemistry, in which imitation of binding entities, such as enzymes and antibodies, is studied [1–3]. In a typical procedure, polymerizable functional monomers are allowed to interact with a suitable template molecule, which can be the molecule of interest or its analog. The resultant complex (either covalent or non-covalent) is then co-polymerized by radical initiation in the presence of a large excess of a cross-linking agent in an inert solvent, which also acts as "porogen" [4]. After the polymerization, the template molecules are washed away, usually by simple extraction techniques, leaving a macroporous rigid polymer with specific cavities for template molecule recognition. Specifically, a "fingerprint" or a "memory" of the template is left in those cavities in a three-dimensional configuration.

In order for catalysis to occur, the MIP binding site must stabilize the transition state of a reaction more than the ground state. Therefore, transition-state analogs of the reaction of interest are often employed as template molecules in order to stimulate catalysis. The MIP catalyst must also bind the products of the reaction with a lower affinity than the intermediates or transition state to ensure turnover [5]. The rigidity of MIP binding sites very often makes it difficult to achieve good turnover rates compared with the more flexible active sites in enzymes, in which conformational changes are adopted to favor product release. The rigidity of MIPs is a consequence of the large excess of cross-linking agent that needs to be used during the pre-polymerization process to preserve the monomer-template shape.

It is well known that catalytic antibodies (abzymes) prepared against a phosphonic ester (a stable transition-state analog for alkaline ester hydrolysis) enhanced the rate of ester hydrolysis by a factor of 10^3–10^4 [6,7]. Catalytic MIPs have also been extensively studied in connection with the biomimetic hydrolysis of *para*-nitrophenyl esters [2,5] where they showed chymotrypsin-like activity. Kawanami and co-workers reported [8] a study of the catalytic hydrolysis of *para*-nitrophenyl acetate by an imprinted polymer that was prepared using *para*-nitrophenyl phosphate as the template (and as a stable transition-state analog of the reaction of interest) and vinylimidazole for the binding site (functionalized monomer). The insoluble salt that was formed on mixing the monomers was allowed to polymerize in the presence of an excess of divinylbenzene as cross-linker. The resulting MIP, after removal of the template, showed a twofold enhancement in rate compared with the control polymer made in the absence of template, and an 85-fold enhancement compared with a control solution at the same pH.

Abbreviations: AIBN, α-azo-iso-butyronitrile; CP MAS, cross-polarization magic-angle spinning; DMSO, dimethyl sulfoxide; EGDMA, ethylene glycol dimethacrylate; EDS, energy dispersive spectroscopy; FT-IR, Fourier transform infrared spectroscopy; GC-FID, gas-chromatography flame-ionization detector; HEMA, 2-hydroxyethyl methacrylate; HMDS, hexamethyldisiloxane; L3, 1,1,3,3,5,5-hexamethyltrisiloxane-1,5-diol; MAA, methacrylic acid; Me_3SiOH, trimethylsilanol; MIPs, molecularly imprinted polymers; NIPs, non-imprinted polymer; RSD, relative standard deviation; SEM, scanning electron microscopy; TMES, trimethylethoxysilane; TMOS, tetramethylorthosilicate; VPY, 4-vinylpyridine.

* Corresponding authors. Present address: Institute of Pharmaceutical Science, King's College London, 150 Stamford Street, London SE1 9NH, UK. Fax: +44 (0)207 848 4785 (V. Abbate).

E-mail addresses: vincenzo.abbate@kcl.ac.uk (V. Abbate), p.g.taylor@open.ac.uk (P.G. Taylor).

0021-9517/$ - see front matter © 2011 Elsevier Inc. All rights reserved.
doi:10.1016/j.jcat.2011.08.019

The most detailed investigation to date of a designed chymotrypsin mimic by means of covalent imprinting was reported by Sellergren and Shea [9], who employed a stable transition-state analog for ester hydrolysis in the form of a chiral phosphonate analog of phenylalanine. To this phosphonate were attached catalytically active phenol and imidazole-containing vinyl monomers through a labile ester linkage. After polymerization in the presence of methacrylic acid and removal of the template, the functional mimics of serine, histidine, and aspartate remained in the sites, which were subsequently used to catalyze ester hydrolysis. Rate enhancements in comparison to non-imprinted polymers were obtained, as well as a very high enantioselectivity, clearly indicating substrate selectivity. In an investigation of the alkaline hydrolysis of an ester, amidine functionalities were employed as the functional monomers using non-covalent interaction for binding and catalysis [2,10]. This work led to the most active imprinted polymer catalyst for ester hydrolysis to date. Michaelis–Menten kinetics was observed, and turnover numbers were measured, although they were relatively low.

Other investigations on MIP-catalyzed reactions include catalysis of carbon—carbon bond formations, such as a Diels–Alder reaction using coordination interaction [11,12], the catalysis of elimination reactions [13,14], and catalysis of oxidation and hydrogen transfer, such as the oxidation of ethylbenzene [15], the hydrogenation of allyl alcohol [16], and the catalytic reduction of ketones [17,18].

To date, there are no reported examples of catalytic MIPs suitable for catalysis in silicon chemistry. In this work, we present the use of MIPs for the catalysis of hydrolysis and condensation of a model alkoxysilane compound, trimethylethoxysilane (TMES), under mild reaction conditions. The catalytic activity of MIPs was compared with non-imprinted polymers (NIPs) as well as to buffer solution at the same pH and temperature. Moreover, MIPs were used to catalyze the biomimetic synthesis of silica–MIP (nano)composites by the hydrolysis and polycondensation of tetramethoxysilane (TMOS). The advantages of using MIPs relative to proteins [19–22] and peptides [23,24] during catalysis at silicon centre include their facile and inexpensive preparation as well as improved stability to heat and organic solvents compared with their biological counterparts.

2. Experimental section

Materials and further experimental conditions are provided in the electronic supplementary section.

2.1. Polymer synthesis

2.1.1. MIPs1–3 and MIP6

For the preparation of MIP1, to a suspension of diphenylsilanediol (template molecule; 0.17 g, ~5% w/w total monomers) in anhydrous DCM (porogen; 9 ml) were added MAA (functional monomer; 1.16 g, ~30% w/w total monomers), EGDMA (cross-linking agent; 2.32 g, ~65% w/w total monomers), and AIBN (radical initiator, 0.028 g, 0.3% w/w total monomers). Upon addition of the acrylate compounds, the heterogeneous mixture became a clear solution, thus allowing the monomer-template interactions. The reaction mixture was degassed with argon and then subjected to two freeze-degas-thaw cycles in order to remove any dissolved oxygen that might inhibit radical polymerization. Subsequently, the mixture was polymerized at approximately 60 °C (oil bath temperature) for 5 h under an argon atmosphere. The monolithic polymer (MIP1) obtained was ground with a mortar and pestle, sieved to collect particles in the range of 50–150 μm size, refluxed in THF overnight using a sohxlet apparatus and finally dried overnight at 50 °C under vacuum. Part of the polymer was kept without extraction for further analyses (MIP1 "crude"). The removal of the template was followed by FT-IR, as well as by solid-state NMR, which no longer showed the peaks corresponding to the template molecules. Comparatively, washing fractions were monitored via GC-FID to assess the efficiency of template removal. MIP2 and MIP3 were synthesized in an identical manner to MIP1 except that MIP3 was photopolymerized under a standard laboratory LW-UV light source at room temperature for 18 h. MIP6 was also prepared in a similar manner as MIP1 except that the template diphenylsilanediol was replaced with the compound 1,1,3,3,5,5-hexamethyltrisiloxane-1,5-diol (L_3). Comparatively, a blank polymer (MIP1b) was prepared in an identical manner to that used for MIP1 but in the absence of any template. CP MAS ^{13}C NMR of MIP1 (100.56 MHz): δ 177.4, 167, 136.4, 63.8, 45.2, and 19 ppm. CP MAS ^{13}C NMR of MIP1b (100.56 MHz): δ 177.5, 167.3, 136.8, 126.4, 63.2, 45.7, and 18.4 ppm. CP MAS ^{13}C NMR of MIP6 (100.56 MHz): δ 177.4, 166.5, 136.9, 126.6, 62.9, 45.8, and 18.4 ppm. FT-IR (KBr disk) of MIP1: 3471, 2991, 1724, 1637, 1454, 1388, 1261, 1163, 957, 816, 756, and 523 cm^{-1}. FT-IR (KBr disk) of MIP1b: 3448, 2959, 1724, 1637, 1454, 1387, 1297, 1261, 1158, 948, 815, and 521 cm^{-1}. FT-IR (KBr disk) of MIP6: 3466, 2993, 1733, 1638, 1458, 1391, 1263, 1163, 957, 881, 815, 755, 656, and 523 cm^{-1}.

2.1.2. MIP4

MAA (0.17 ml, 2 mmol), EGDMA (10 mmol, 1.9 ml), the template **1** (0.161 g, 0.5 mmol), and AIBN (0.02 g, 0.125 mmol) were dissolved in anhydrous DMSO (3 ml). The polymerization mixture was purged with argon and subjected to three freeze–thaw-degas cycles; subsequently, thermally initiated radical polymerization was conducted at approximately 60 °C (oil bath temperature) for 20 h under an argon atmosphere. The polymer was ground with a mortar and pestle, sieved to collect particles in the range of 50–150 μm size, sohxlet extracted overnight in methanol, and dried in vacuo at 50 °C overnight. MIP4 was subjected to an extensive DMSO wash prior to extraction, in order to quantitatively remove the template. An aliquot of the polymer was kept without extraction for further analyses (crude MIP4). CP MAS ^{13}C NMR of MIP4 (100.56 MHz): δ 177.1, 167.5, 136.8, 126.4, 62.8, 45.6, and 18.4 ppm. FT-IR (KBr disk) of MIP4: 3456, 2991, 1728, 1637, 1456, 1390, 1261, 1161, 957, 879, 816, 755, and 521 cm^{-1}.

2.1.3. MIP5

Monomers HEMA (0.180 ml, 1.5 mmol,) and VPY (0.053 ml, 0.5 mmol), EGDMA (1.9 ml, 10 mmol), template **1** (0.161 g, 0.5 mmol), and AIBN (0.02 g, 0.125 mmol) were dissolved in anhydrous DMSO (3 ml). The polymerization mixture was purged with argon and subjected to three freeze–thaw-degas cycles; subsequently, thermally initiated radical polymerization was conducted at approximately 60 °C (oil bath temperature) for 20 h and then at approximately 65 °C for 24 h to fully cure the material. The polymer was ground, sieved to collect particles in the range of 50–150 μm size, subjected to an extensive DMSO wash in order to efficiently remove the template, and dried overnight under vacuum 50 °C. A fraction of the latter was also sohxlet extracted in methanol overnight, in order to wash out unreacted material and possibly some residual template, and finally dried in vacuo overnight at 50 °C. An aliquot of the polymer was kept without further treatment for analysis (MIP5 crude). The removal of the template was followed by FT-IR as well as solution and solid-state NMR. CP MAS ^{13}C NMR of MIP5 (100.56 MHz): δ 177.1, 167.2, 150.0, 136.7, 126.8, 62.7, 45.7, and 18.1 ppm. FT-IR (KBr disk) of MIP5: 3436, 2926, 1733, 1644, 1458, 1389, 1257, 1158, 954, 835, 754, and 475 cm^{-1}.

2.2. Hydrolysis and condensation study of alkoxysilane

The reactions were formulated with approximately 4:1 alkoxysilane (TMES) (80 mg) to polymer catalyst (20 mg) weight ratio in 0.5 g of 100 mM tris–HCl buffered Milli-Q water, pH 7.0, containing 20 mM NaCl. The closed (screw capped) reactions were conducted in inert glass vials at 25 °C with magnetic stirring for desired reaction time. The reaction products were isolated and quantitatively analyzed by GC-FID. Results are expressed as the average of triplicate measurements; RSD% (relative standard deviation, i.e., standard deviation/average) ranged between 0.3% and 3%, thus accounting for good reproducibility of the quantitative measurements. Prior to analysis, the aqueous reactions were extracted with 1 ml of THF in the presence of NaCl and filtered through a Whatman Autovial® 12.

2.3. Silanol condensation study

The reactions were formulated with approximately 4:1 silanol (Me_3SiOH) (80 mg) to polymer catalyst (20 mg) weight ratio in 0.5 mL of 100 mM tris–HCl buffered Milli-Q water, pH 7.0, containing 20 mM NaCl. The closed (screw capped) reactions were conducted in inert glass vials at 25 °C with magnetic stirring for 24 h. The reaction products were isolated and quantitatively analyzed by GC-FID. RSD% ranged between 0.3% and 3%, thus accounting for good reproducibility of the quantitative measurements. Prior to analysis, the aqueous reactions were extracted with 1 ml of THF in the presence of NaCl and filtered through a Whatman Autovial® 12, 0.45-μm Teflon® filter.

2.4. Biomimetic MIPs-mediated synthesis of silica

The reactions were formulated with approximately 4:1 TMOS (40 mg) to imprinted polymer (10 mg) weight ratio in 0.4 ml of 100 mM tris–HCl buffered Milli-Q water, pH 7.0, containing 20 mM NaCl. The closed (screw capped) reactions were conducted in inert glass vials at 25 °C with magnetic stirring for 3 days. The aqueous reactions were extracted with 1 ml of THF in the presence of NaCl to remove soluble oligomers. The isolated solid materials were dried under vacuum and analyzed via SEM–EDS and FT-IR.

2.5. Control reactions

Experiments conducted in the absence of a polymer are defined as negative control reactions, whereas NIPs (non-templated materials, i.e., blank polymers) were used to study non-specific catalysis.

3. Results and discussion

3.1. Polymer preparation and characterization

A series of imprinted polymers was synthesized (Table 1) in order to investigate their ability to catalyze *in vitro* siloxane bond formation. All the polymers were prepared using non-covalent self-assemblies of the templates with the functional monomers prior to polymerization. Although the non-covalent approach would not allow the generation of "stoichiometrically positioned" reactive functionalities in the imprinted cavities (i.e., a 1:1 ratio between monomer and template), the method offers advantages such as facile and efficient removal of the template molecules after the polymerization, compared with that for covalent imprinting. As detailed in Table 1, various types of functional monomer(s) and templates were employed. Specifically, these were mixed with an excess of cross-linking agent in the appropriate porogen, and the radical initiator α-azoiso-butyronitrile (AIBN) was added. Ethylene glycol dimethacrylate (EGDMA) was adopted as the cross-linking agent due to its established use in this research area [1,2,4,25,26]. In a typical procedure, the reagents were mixed, degassed with 2–3 freeze-degas-thaw cycles and/or purging with argon gas for 10 min, and finally thermally or photochemically polymerized by free-radical polymerization. The transparent solution slowly turned to gel and eventually solidified to afford a rigid monolith. After breaking the glass container, the polymer was manually ground with a mortar and pestle and sieved to collect particles in the range 50–150 μm. Subsequently, the MIP was washed using a sohxlet apparatus to remove the template molecule and unreacted monomers, and finally dried in a vacuum oven. Polymers were stored in a desiccator at room temperature. Blank (i.e., non-imprinted) polymers were synthesized and treated in an identical manner to the corresponding MIPs but in the absence of any template. The physico-chemical properties of the MIPs were investigated in the solid state, as they are rigid insoluble materials. Specifically, the polymers were analyzed via solid-state NMR, FT-IR, and SEM–EDS analyses. The soxhlet-extracted fractions were kept for further analysis to study the removal and stability of templates under the described conditions.

The ^{13}C CP MAS NMR spectrum of copolymer MIP1 (Fig. S2) shows peaks at around 180 and 170 ppm, which represent the carbonyl moieties corresponding to reacted and unreacted (i.e., RCHCO and C═C—CO) acrylates, respectively. From the peak area ratios, it is possible to estimate the extent of polymerization and, therefore, the amount of unreacted double bonds left in the material after the preparation of the MIP [1,27,28]. Although some unreacted acrylates always remained entrapped in the polymer matrix, even after exhaustive washing of the solid, the results show a large degree of polymerization. This is essential to provide a highly cross-linked rigid framework, which allows the chemical and spatial arrangement that is generated prior to polymerization to be maintained. Peaks in the region 136–126 ppm also denote the presence of double bonds which remained unreacted after polymerization. Specifically, they belong to the acrylic carbons of acrylates from monomer and cross-linking agents. The peak at around 63 ppm is attributed to the methylene carbons of EGDMA, whereas the sharp singlet appearing at around 45 ppm corresponds to the formation of the CH of the acrylic carbons upon saturation of the double bonds, as expected from radical polymerization. Finally, a peak at around 18 ppm is attributable to the α-CH_3 of the acrylates. CP MAS NMR was therefore shown to be a useful tool for providing qualitative information about the imprinted polymers' composition.

Infrared spectra of insoluble MIPs are easily obtained from KBr pellets of the polymers [29]. The FT-IR spectrum of MIP1 (Fig. S3) shows bands at around 1637 and 950 cm^{-1}, which provide information about the extent of unreacted double bonds in the material due to olefinic moieties. As already observed in the NMR data, the MIPs prepared here show a high degree of free-radical polymerization, with little unreacted acrylates remaining in the polymer matrix. A clear band in the region of 1700 cm^{-1} is attributed to carbonyl groups derived both from the esters and the carboxylic acids. The broad band at around 3300–3500 cm^{-1} is due to OH stretching. Generally, a band at 3300 cm^{-1} is attributed to hydrogen-bonded dimers of carboxylic acids, whereas a peak at 3440 cm^{-1} is attributed to isolated (free) carboxylate groups. Although our spectra show a rather broad OH band, making it difficult to distinguish between isolated versus hydrogen-bonded carboxylates, strong absorbances were observed at higher wavelengths (generally, approximately 3440–3460 cm^{-1}), with only small inflections at around 3300 cm^{-1}. This indicates the presence of free carboxylic acid that should be available to react and catalyze reactions upon incubation with the substrate, along with a small amount of hydrogen-bonded cyclic dimers that may not be available for the catalytic activity. Other characteristic bands are at 2900–3000 cm^{-1}, which

Table 1
Composition of MIPs prepared in this study.

MIP	Template	Porogen	Functional monomer	Cross-linker	Initiator	(°C)	Time (h)	Extraction
1–2	Diphenylsilanediol	DCM	MAA	EGDMA	AIBN	60	5	THF
1b	/	DCM	MAA	EGDMA	AIBN	60	5	THF
3	Diphenylsilanediol	DCM	MAA	EGDMA	AIBN	RT	18	THF
4	Compound **1**	DMSO	MAA	EGDMA	AIBN	60	20	DMSO/MeOH
5	Compound **1**	DMSO	HEMA/VPY	EGDMA	AIBN	60–65	44	DMSO/MeOH
6	L_3	DCM	MAA	EGDMA	AIBN	60	5	THF

can be assigned to the CH stretches of the aliphatic CH; around 1450 cm^{-1}, attributed to the —O—CH_2 bending; 1263 cm^{-1}, due to C—O bend; an intense peak at 1163 cm^{-1} belonging to the ester systems; 955 cm^{-1}, C—CH_3 rocking; and finally in the 750–850 cm^{-1} region, attributable to CH_2 rocking. FT-IR represented a rapid and powerful technique to gain information about chemical and structural polymer characteristics.

Surface analyses were also carried out; specifically, scanning electron microscopy (SEM) (Fig. 1) and electron dispersive spectra (EDS) (Fig. S4) were acquired in order to investigate the morphology and the surface elemental composition of the polymers, respectively.

Generally, the MIPs prepared consisted of tightly packed overlapping irregularly shaped surface particles that ranged in size from approximately 200 to 660 nm. The inhomogeneous morphology is due to the polymerization method adopted, or possibly due to the grinding and sieving processes. The surfaces appeared sponge-like and porous, as can be seen at higher magnification. These "open channels" represent the space originally occupied by the solvent (porogen) molecules, which is evaporated during the work up. The porosity of the MIPs is very important, as it allows the fast exchange of substrates in and out of the polymers. A typical EDS spectrum of the particles (Fig. S4) shows two main peaks belonging to oxygen and carbon in the polymeric backbone (although some carbon also derives from the support). Additionally, the tiny peak (approximately 0.1%) corresponding to silicon may be due to glass residues in the solid, or possibly some residual silicon-based template entrapped in the polymer.

3.2. Molecular imprinted polymer (MIP)-catalyzed hydrolysis and condensation of trimethylethoxysilane

Polymers were evaluated for their ability to promote siloxane bond formation under ambient conditions. The investigated functional monomer was MAA, since it is capable of hydrogen bonding and the most widely used compound in non-covalent imprinting approaches. MIP1 was synthesized in the presence of diphenylsilanediol as the template and using anhydrous DCM as the porogen. The silanediol was not very soluble in DCM; however, upon addition of MAA and EGDMA, the mixture immediately turned clear, as a result of the appropriate self-assembly. Solubilization of the template upon monomer addition may be a positive sign of interaction, and therefore complexation, of the participating species. A pre-arrangement similar to that shown in Fig. 2 was expected. After removal of the template, imprinted cavities complementary to the template were thought to be formed, along with several carboxylic acid residues embedded in the matrix due to the excess monomer used in the synthetic approach.

High excess of MAA was necessary to fully complex all the template moieties in order to generate sufficient imprinted

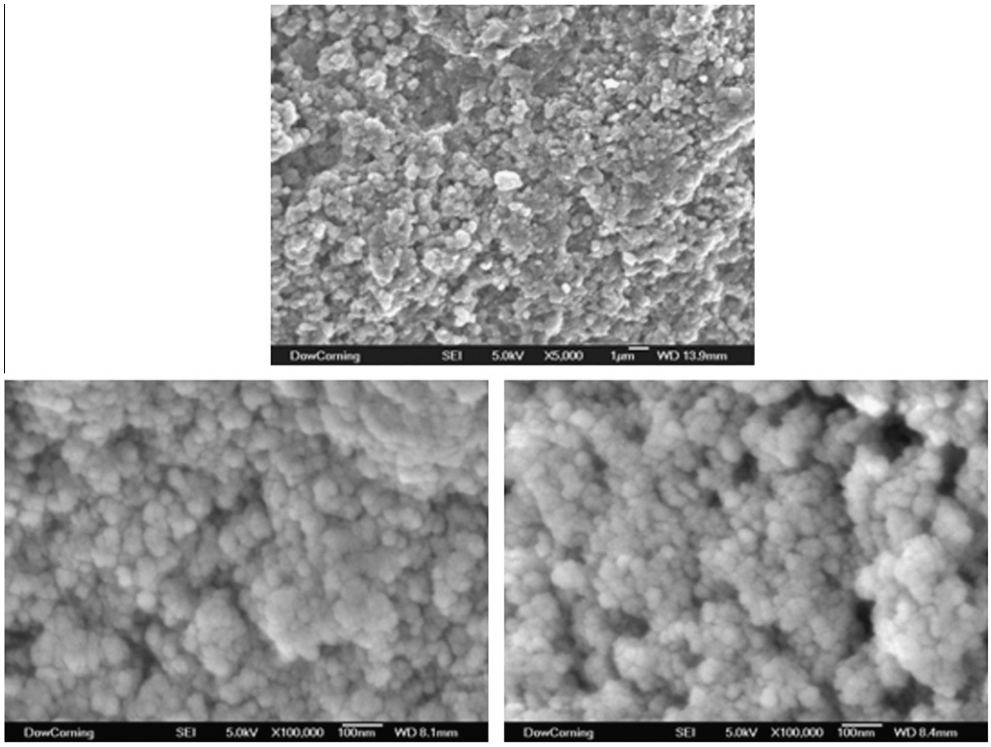

Fig. 1. Scanning electron micrographs of: MIP1 (top); MIP5 (bottom left); and MIP4 (bottom right).

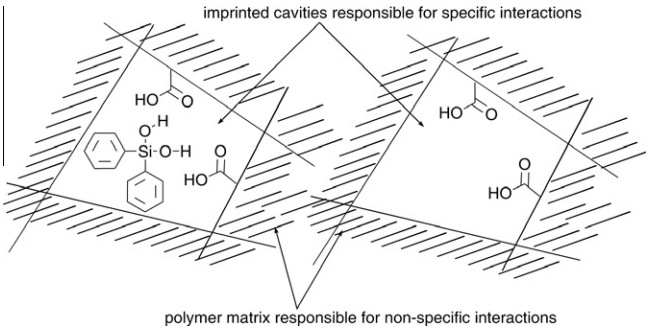

Fig. 2. Proposed arrangements in the MIP1 imprinted cavities before (left) and after (right) template removal.

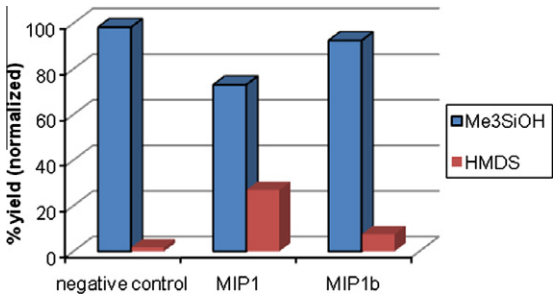

Fig. 3. MIP1 and MIP1b condensation study of Me_3SiOH in tris-buffered water after 24 h at 25 °C.

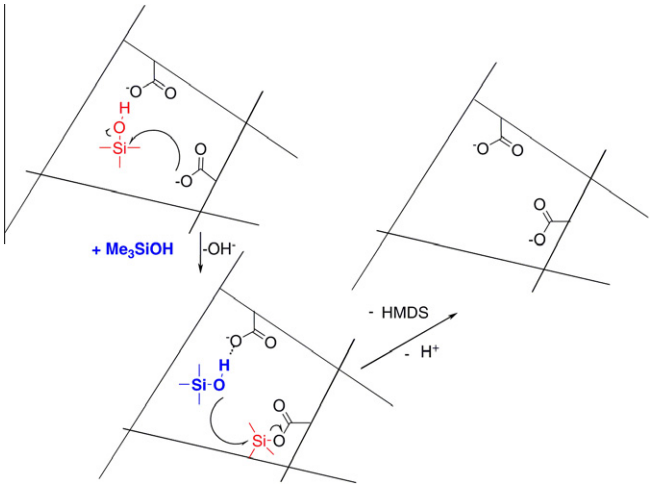

Fig. 4. Proposed mechanism for the MIP1-catalyzed siloxane bond formation.

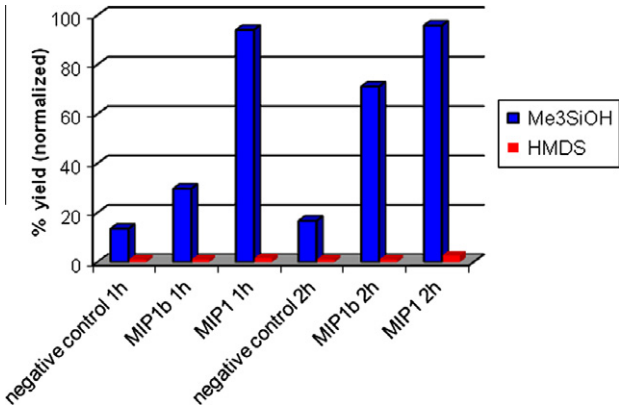

Fig. 5. MIP1- and MIP1b-catalyzed hydrolysis and condensation study of Me_3SiOEt in tris-buffered water at 25 °C. Mass balance is not 100% here as hydrolysis of TMES was not complete in this study.

nanocavities. Standard recipes for MIP preparation generally employ a 1:4:20 monomer:template:cross-linker molar ratios [26], and this procedure was adopted for the preparation of MIPs4–5. However, such a low amount of functional monomer was observed to be insufficient to generate efficient imprinted catalysts for the condensation of the model silanol (not shown). Although we did not employ the usual high degree of cross-linking agent for MIPs1–3 and MIP6, the process was still believed to potentially generate stable imprinted cavities, leading to siloxane biomimetic catalysis. For MIPs1–3, diphenylsilanediol was chosen as the pseudo-transition state analog for the alkoxysilane hydrolysis and condensation reaction. Diphenylsilanediol contains two Si—O bonds, to some extent mimicking the transition state of our model reaction, i.e., the hydrolysis of TMES to produce Me_3SiOH, followed by condensation into HMDS. In the condensation reaction, it is assumed that a pentacoordinate silicon intermediate is generated during the nucleophilic attack of the oxygen of a molecule of silanol on the silicon atom of the second silanol molecule. The two hydroxyl moieties of the imprinted molecule (template) can interact through hydrogen bonds to the MAA carboxylates, while the phenyl rings can participate in non-polar interactions with the apolar region of the polymer matrix. Although the interactions described are rather weak, the totality of the bonding network generated should be strong enough to develop nano-imprinted tailored cavities. Furthermore, the surface reactive carboxylate groups would be strategically located so that an artificial active site somewhat mimicking that of pepsin or lysozyme was generated. These two enzymes were shown to promote siloxane bond formation [20], therefore carboxylate groups may be good candidates for our MIP-catalysis studies.

The removal of the template was followed by solid-state NMR and EDS analysis, which showed none or minimal residual silicon to be present. The solution NMR of the residual sohxlet-extracted fraction confirmed, even if only in a qualitative way, the presence of template. From the NMR spectra (not shown), it was possible to observe that diphenylsilanediol did undergo a small amount of condensation, possibly catalyzed by methacrylic acid. Nevertheless, the major peak in the ^{29}Si NMR spectrum of the extract was due to diphenylsilanediol, suggesting that imprinted cavities complementary to the original template molecule were generated.

Fig. 3 shows that MIP1 was observed to catalyze the condensation of Me_3SiOH into HMDS in tris-buffered water (pH 7.0) over 24 h to a greater extent than a control solution at the same pH and a control blank polymer (MIP1b) synthesized in an identical manner but in the absence of template. Substantial hydrolysis of TMES to give Me_3SiOH was also observed with the negative control and NIP reactions over 24 h. In fact, we were not able to differentiate between polymer-mediated versus chemically catalyzed hydrolysis over this time period. Notably, no condensation product was observed in the absence of polymers, and very little condensation product was formed in presence of the NIP. The greater activity of the imprinted versus non-imprinted polymer was therefore assumed to be due to the presence of imprinted cavities in the MIP. Condensation observed in the blank polymer could be attributed to non-specific catalysis mediated by randomly positioned MAA residues in the bulk material. A mechanism can be hypothesized where the two acidic residues on the cavity surfaces are involved (Fig. 4). The imprinted cavities are suitable for accommodation of the Me_3SiOH molecule. The substrate is anchored and stabilized through hydrogen bonding with a MAA residue plus non-polar interactions with the bulk polymer matrix. Subsequently, the silanol molecule undergoes nucleophilic attack from

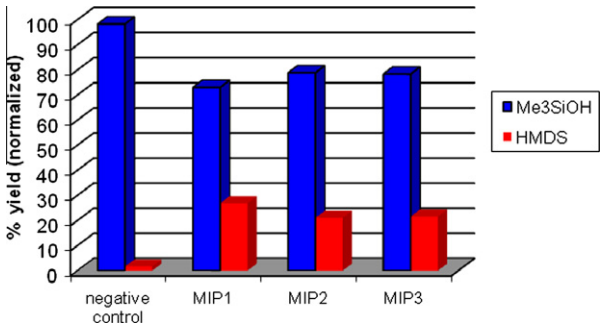

Fig. 6. MIPs1–3 condensation study of Me_3SiOH in aqueous media after 24 h at 25 °C.

the second carboxylate MAA residue. In the second step, another Me_3SiOH molecule, with more nucleophilic oxygen due to hydrogen bonding with the MAA, can attack the methacryloyltrimethylsilyl intermediate to form HMDS. According to this hypothesis, the MIP should act as a true catalyst, enhancing the rate but remaining unaltered after the reaction. The rigidity and insolubility of the polymer make it mechanically stable and easy to remove from the reaction mixture (by simple filtration). These properties, together with the better stability of the MIPs toward factors such as pH and temperature, render these polymers more suitable for industrial applications compared with soluble catalysts and biocatalysts.

The hydrolysis and condensation of TMES were also followed over a short time period (i.e., 1–2 h) in the presence of MIP1 and the control MIP1b (Fig. 5).

TMES was not observed to be fully hydrolyzed over the time course studied; however, only the hydrolysis (Me_3SiOH) and condensation (HMDS) product yields are presented, and the mass balance was fully completed by the residual starting material (TMES). Although the imprinted polymer MIP1 catalyzed the hydrolysis of TMES faster than the non-imprinted (blank) polymer MIP1b, substantial hydrolysis was also observed in the presence of MIP1b compared with a control buffer solution. It appears that randomly distributed MAA residues in the polymer matrix, rather than the imprinted cavities, promoted the hydrolysis. While TMES should be small enough to be accommodated into the cavities, it lacks the silanol functionality to act as a hydrogen bond donor. Therefore, the recognition of the "artificial active site" could be partially lost. To the best of our knowledge, this is the first case of a biomimetic siloxane bond formation mediated by an artificial MIP-based microreactor.

To evaluate the reproducibility of the catalytic activity of the polymer MIP1, it was prepared again in an identical manner to give a polymer MIP2. Another polymer identical to MIP1 was also synthesized but adopting the photolytic free-radical polymerization procedure. In this way, a polymer MIP3 was obtained. MIP2 and MIP3 were tested in the Me_3SiOH–HMDS model condensation reaction.

The results are illustrated in Fig. 6 and demonstrate that it was possible to replicate the experiments with minimal variations in catalytic activity, which were attributed to polymer surface irregularity or technical/instrumental error. The results show that the catalytic properties of MIP1 did not vary between thermally cured materials compared with those obtained by UV-initiated free-radical polymerization. Several groups [30–32] reported the advantages of photolytic versus thermal free-radical polymerization. The former is generally conducted at low temperatures, thus allowing the use of thermally unstable substrates, whereas heat-induced free-radical polymerization is preferred when photolabile compounds have to be used in the reaction. Moreover, it is believed that polymers prepared by the UV method at low temperatures will show better recognition properties during the separation of the analyte from complex mixtures; conversely, thermally polymerized materials showed excellent activity when used as catalysts. In our study, both types of polymerization seemed to produce materials with almost identical catalytic activities.

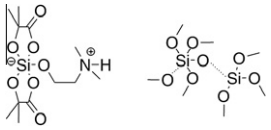

Fig. 8. Comparison between compound 1 (left) and the proposed transition-state intermediate of TMOS hydrolysis/condensation (right).

To get more insight into the nature of the hypothesized artificial active site and to further consolidate the proposed catalytic mechanism, another polymer, MIP6, was prepared. MIP6 was also a MAA–EGDMA-based imprinted co-polymer. It was synthesized in the presence of the template L_3. The surface-binding cavities were expected to be similar to those in MIP_1 and MIP_2, except for the distance between the two carboxylic acid residues (Fig. 7).

Indeed, computer simulations of the minimized structures of diphenylsilanediol and L_3 suggest a distance between the two hydrogen bonding participating hydroxyls of ~2.7 Å and ~7.2 Å, respectively. MIP6 did not catalyze the condensation of HMDS to any additional extent compared with its blank counterpart MIP1 (not shown). The greater distance between the two MAA residues in the cavities may account for the lack of catalytic activity. Although there would still be two reactive carboxylates in the imprinted holes, these may not be oriented in the correct distance and proximity to cooperate during the siloxane bond catalysis, as observed in the case of MIP1.

3.3. MIP-mediated biomimetic synthesis of silica

To assess whether the MIPs could also be used as catalysts for the biomimetic synthesis of silica under mild reaction conditions, several imprinted and non-imprinted polymers were incubated in a neutral aqueous medium in the presence of TMOS. In this study, we evaluated the catalytic efficiency both of the "high functional monomer recipe" (MIP1), as well as the "standard" MIP preparation procedure (MIP4–5, i.e., 1:4:20 template:monomer:cross-linker molar ratios). MIP4 was prepared using MAA as the functional monomer in the presence of the pentacoordinate silicon compound **1** as the template species, given the similarity of this compound to

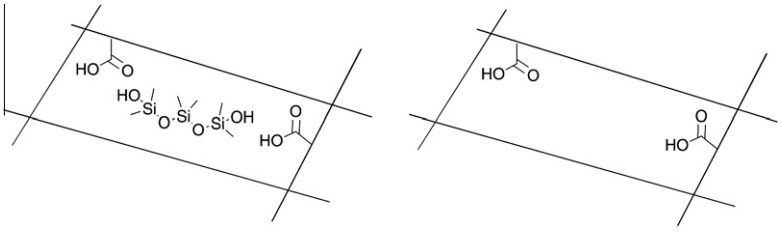

Fig. 7. Schematic representation of the MIP3 imprinted cavity arrangements before (left) and after (right) template removal.

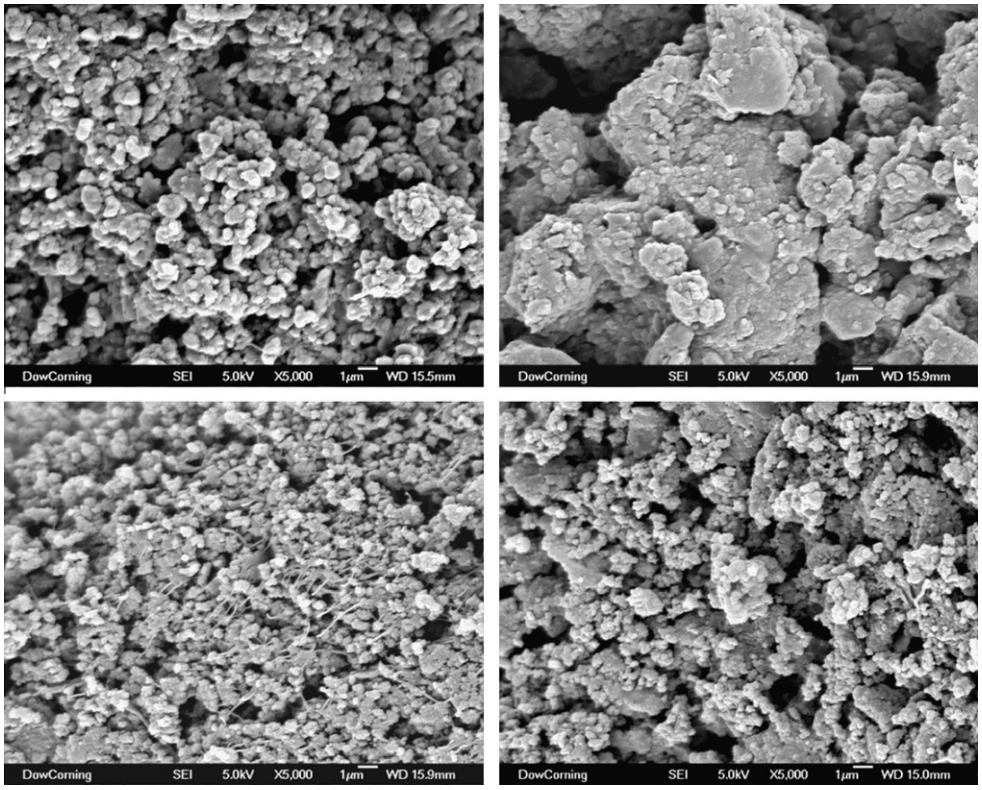

Fig. 9. Scanning electron micrographs of: MIP1/silica composite (top left), MIP1b/silica composite (top right); MIP4 (bottom left); MIP5 (bottom right).

Table 2
EDS data of MIP/silica composites.

	%C	%O	%Si	%Na	%Cl
MIP_1	71	12	17	0	0
MIP_{1b}	80	16	1	1	1
MIP_4	74	16	8	0	2
MIP_5	72	9	17	1	1

the transition-state species of the reaction of interest, as depicted in Fig. 8.

This template was chosen as a pseudo-transition state analog because it resembles the transition state or intermediate of a Si—O bond cleavage and formation reaction, during which it was supposed that pentacoordinate silicon species is formed [33]. This has been confirmed by solid-state NMR studies on diatoms [34], where silicon peaks belonging to a hypervalent domain were found. Removal of the template was followed by solution and solid-state NMR studies, as well as by FT-IR and electron dispersion spectra. The pentacoordinate silicon compound was quantitatively removed after an extensive DMSO wash and showed no sign of decomposition under polymerization conditions (not shown). MIP5 was synthesized again using compound **1** as the print molecule but employing two different functional monomers to complex the template during the pre-polymerization complex. Specifically, a HEMA–VPY system was selected in order to develop biomimetic catalysts for the polycondensation of TMOS leading to particulate amorphous silica. HEMA was chosen as a serine-mimic, because serine proteases such as trypsin and lipases were found to catalyze siloxane bond formation [19,20,35] and silica precipitation [21]. The VPY was chosen because the pyridine may render the hydroxyl functionalities more reactive (nucleophilic) via hydrogen bonding between the pyridine nitrogen and the hydroxyl of the HEMA, leading to a more efficient siloxane bond catalysis. Thus by mixing HEMA and VPY, we attempted to create an artificial active site somewhat similar to those of serine proteases.

The silica precipitation reactions were formulated with approximately 4:1 monomer to catalyst weight ratio and conducted in tris-buffered water (pH = 7.0), at room temperature and in inert glass vials. After 3 days, the mixtures were extracted with THF to remove unreacted monomers/oligomers, dried under vacuum, and analyzed via SEM–EDS (Fig. 9 and Table 2) and FT-IR (Fig. 10). Since the MIPs are white insoluble materials, the study did not allow following the precipitation of silica with time. Therefore, it was decided to conduct the reactions for 3 days and analyze the solid products, which obviously contained organic material (MIP), but also inorganic silica, as shown in the EDS data (Table 2) and in the IR spectrum (Fig. 10), where both signals from organic (MIPs) and inorganic (silica) components were evident. In the IR spectrum, it is possible to note a broad band in the region of 3300–3600 cm^{-1} due to carboxylate groups, as well as a strong band at ~1700 cm^{-1} due to the presence of carbonyl moieties of the monomers; in addition, a broad band was observed at around 1000–1200 cm^{-1}, which can be attributed to the partial overlap of Si—O—Si stretching (normally occurring at 1090 cm^{-1}) and the ester system absorption (1163 cm^{-1}). MIP1 (diol template) and MIP5 (template **1**) composites appeared as tightly agglomerated, rather irregular particles ranging from 160 to 800 nm in size. MIP4 (template **1** with HEMA VPY) composite appeared as irregular shaped particles ranging from 250 to 600 nm in size, together with some particles that had a fibrous appearance, and they were larger (up to 2.5 μm in length). Possibly, the filamentous particles may consist of silica deposited onto the irregular, MIP-based, particles (see also Fig. 3).

The non-imprinted MIP1b also precipitated silica, although there was no particular control in the morphology compared with the imprinted polymers, and the amount of silicon detected on the surface was considerably lower. From the EDS data, it was only

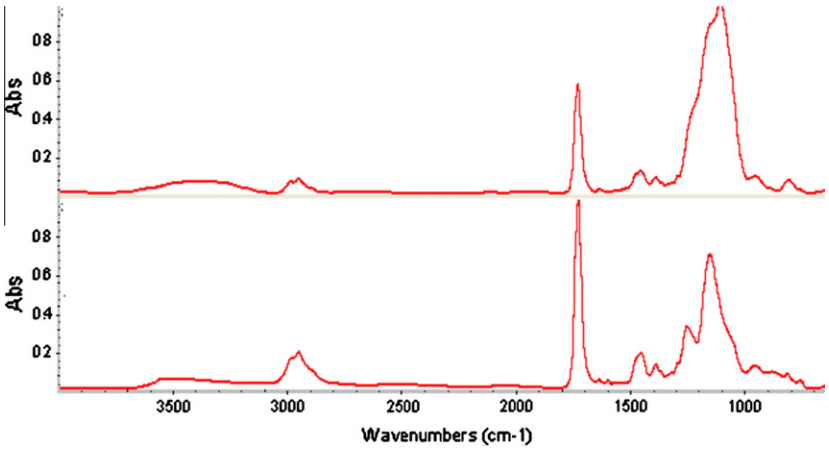

Fig. 10. FT-IR spectra of MIP4–silica (top) and MIP5–silica (bottom) composites.

possible to qualitatively estimate the elemental surface composition, as the carbon content was assumed to be the sum of the MIP and carbon stub (i.e., SEM sample holder) contributions. EDS is a standardless, semi-quantitative analysis. The primary aim of this experiment was therefore to estimate the atomic composition of the surface of the samples and to assess the presence of inorganic silica due to successful polycondensation of the starting tetraalkoxysilane.

The results show that it is possible to catalyze the precipitation of amorphous silica with some control of particle morphology in the presence of MIPs under mild reaction conditions. The method offers a route to synthesizing novel affinity stationary phases and inorganic/organic hybrid materials. While we observed catalysis of Si—O—Si bond formation with the model Me_3SiOH compound only by employing MIPs1–3 (high functional monomer level), it is worth noting that polycondensation of silica could be attained even in the presence of MIPs (and NIPs) synthesized via "conventional" MIPs preparation; this was attributed to the more facilitated process of Si—O—Si bond formation in polysilicic acid species at neutral pH as opposed to the Me_3SiOH condensation system. Further studies are being conducted in our laboratory to extend the use of MIPs in silicon chemistry, including the use of different mono- and dialkoxy-based monomers, and such a detailed characterization of these materials will be reported in a further paper.

4. Conclusion

Several MIPs were prepared, characterized, and tested for their ability to catalyze the cleavage and formation of siloxane bonds under mild reaction conditions. High-MAA content MIPs prepared either via thermopolymerization or photopolymerization were observed to catalyze the condensation of a model silanol (Me_3SiOH) to the corresponding disiloxane (HMDS). The catalysis was assumed to occur in the imprinted cavities. Conversely, the hydrolysis of the model ethoxysilane occurred both in the imprinted and in the non-imprinted materials, and it was thus attributed to random, non-specific functionalities embedded in the polymeric matrix. Moreover, it was shown that selected MIPs were able to hydrolyze TMOS and precipitate particulate amorphous silica under ambient conditions. MIPs thus represent a novel synthetic alternative to their biological counterparts for molecular recognition at silicon centre. Although we have reported that enzymes can function as catalysts during organosilicon biotransformation [19,20], MIPs possess several advantages over bio-catalysts. These synthetic polymers are more stable toward mechanical pressure, making them more suitable, for example, as stationary phases. Also, MIPs are much more stable to pH changes, heat, and organic solvents compared with peptides and proteins. Therefore, we envisage that MIPs may represent a powerful novel class of catalysts for (organo)silicon chemists and the silicon industry in the near future.

Acknowledgments

This work was generously supported by Dow Corning Corporation (Midland, MI, USA). The solid-state NMR measurements were carried out at the EPSRC solid-state NMR service in Durham (UK).

Appendix A. Supplementary material

Supplementary data associated with this article can be found, in the online version, at doi:10.1016/j.jcat.2011.08.019.

References

[1] B. Sellergren, Molecularly Imprinted Polymers: Man Made Mimics of Antibodies and Their Applications in Analytical Chemistry, Elsevier, Amsterdam, 2001.
[2] G. Wulff, Chem. Rev. 102 (2002) 1–28.
[3] G. Wulff, B.O. Chong, U. Kolb, Angew. Chem. Int. Ed. 45 (2006) 2955–2958.
[4] M.T. Komiyama, T. Mukawa, H. Asanuma, Molecular Imprinting, WILEY-VCH Verlag GmbH & Co. KGaA, Weinheim, 2003.
[5] C. Alexander, L. Davidson, W. Hayes, Tetrahedron 59 (2003) 2025–2057.
[6] R.A. Lerner, S. J Benkovic, P.G. Schultz, Science 252 (1991) 659–667.
[7] P.G. Schultz, Angew. Chem. Int. Ed. 101 (1989) 1336–1348.
[8] Y. Kawanami, T. Yunoki, A. Nakamura, K. Fujii, K. Umano, H. Yamauchi, K. Masuda, J. Mol. Catal. Chem. 145 (1999) 107–110.
[9] B. Sellergren, K.J. Shea, Tetrahedron Asymm. 5 (1994) 1403–1406.
[10] B. Sellergren, R.N. Karmalkar, K.J. Shea, J. Org. Chem. 65 (2000) 4009–4027.
[11] J. Matsui, I.A. Nicholls, I. Karube, K. Mosbach, J. Org. Chem. 61 (1996) 5414–5417.
[12] I.A. Nicholls, J. Matsui, M. Krook, K. Mosbach, J. Mol. Recognit. 9 (1996) 652–657.
[13] X.C. Liu, K. Mosbach, Macromol. Rapid Commun. 19 (1998) 671–674.
[14] R. Muller, L.I. Andersson, K. Mosbach, Macromol. Rapid Commun. 14 (1993) 637–641.
[15] A.A. Efendiev, Macromol. Symp. 80 (1994) 289.
[16] C.U. Pittman Jr., C.E. Carraher Jr., M. Zeldin, J. Sheats, B.M. Culbertson, Metal-Containing Polymeric Materials, Plenum Press, New York, 1996.
[17] F. Locatelli, P. Gamez, M. Lemaire, J. Mol. Catal. Chem. 135 (1998) 89–98.
[18] K. Polborn, K. Severin, Chem. Commun. (1999) 2481–2482.
[19] V. Abbate, A.R. Bassindale, K.F. Brandstadt, R. Lawson, P.G. Taylor, Dalton Trans. 39 (2010) 9361–9368.
[20] V. Abbate, A.R. Bassindale, K.F. Brandstadt, P.G. Taylor, J. Inorg. Biochem. 105 (2011) 268–275.
[21] A.R. Bassindale, P.G. Taylor, V. Abbate, K.F. Brandstadt, J. Mater. Chem. 19 (2009) 7606–7609.
[22] K. Shimizu, J. Cha, G.D. Stucky, D.E. Morse, Proc. Natl. Acad. Sci. USA 95 (1998) 6234–6238.

[23] N. Kroger, R. Deutzmann, M. Sumper, Science 286 (1999) 1129–1131.
[24] J.N. Cha, K. Shimizu, Y. Zhou, S.C. Christiansen, B.F. Chmelka, T.J. Deming, G.D. Stucky, D.E. Morse, Mater. Res. Soc. Symp. Proc. 599 (2000) 239–248.
[25] G. Wulff, Angew. Chem. Int. Ed. 34 (1995) 1812–1832.
[26] B. Sellergren, K.J. Shea, J. Chromatogr. 635 (1993) 31.
[27] T. Hjertberg, Macromolecules 23 (1990) 3080–3087.
[28] R.V. Law, D.C. Sherrington, C.E. Snape, I. Ando, H. Kurosu, Macromolecules 29 (1996) 6284–6293.
[29] L.J. Bellamy, The Infrared Spectra of Complex Molecules, Halsted Press, Berlin, 1976.
[30] D.J. O' Shannessy, B. Ekberg, K. Mosback, Anal. Biochem. 177 (1989) 144–149.
[31] S.A. Piletsky, I. Mijangos, A. Guerreiro, E.V. Piletska, I. Chianella, K. Karim, A.P.F. Turner, Macromolecules 38 (2005) 1410–1414.
[32] D.A. Spivak, Adv. Drug Deliv. Rev. 57 (2005) 1779–1794.
[33] Y. Zhou, K. Shimizu, J.N. Cha, G.D. Stucky, D.E. Morse, Angew. Chem. Int. Ed. 38 (1999) 780–782.
[34] S.D. Kinrade, A.M.E. Gillson, C.T.G. Knight, J. Chem. Soc. Dalton Trans. (2002) 307–309.
[35] A.R. Bassindale, K.F. Brandstadt, T.H. Lane, P.G. Taylor, J. Inorg. Biochem. 96 (2003) 401–406.